Magnetic resonance imaging of benign prostatic hyperplasia

Serkan Guneyli
Emily Ward
Stephen Thomas
Ambereen Nehal Yousuf
Igor Trilisky
Yahui Peng
Tatjana Antic
Aytekin Oto

ABSTRACT

Benign prostatic hyperplasia (BPH) is a common condition in middle-aged and older men and negatively affects the quality of life. An ultrasound classification for BPH based on a previous pathologic classification was reported, and the types of BPH were classified according to different enlargement locations in the prostate. Afterwards, this classification was demonstrated using magnetic resonance imaging (MRI). The classification of BPH is important, as patients with different types of BPH can have different symptoms and treatment options. BPH types on MRI are as follows: type 0, an equal to or less than 25 cm³ prostate showing little or no zonal enlargements; type 1, bilateral transition zone (TZ) enlargement; type 2, retrourethral enlargement; type 3, bilateral TZ and retrourethral enlargement; type 4, pedunculated enlargement; type 5, pedunculated with bilateral TZ and/or retrourethral enlargement; type 6, subtrigonal or ectopic enlargement; type 7, other combinations of enlargements. We retrospectively evaluated MRI images of BPH patients who were histologically diagnosed and presented the different types of BPH on MRI. MRI, with its advantage of multiplanar imaging and superior soft tissue contrast resolution, can be used in BPH patients for differentiation of BPH from prostate cancer, estimation of zonal and entire prostatic volumes, determination of the stromal/glandular ratio, detection of the enlargement locations, and classification of BPH types which may be potentially helpful in choosing the optimal treatment.

Benign prostatic hyperplasia (BPH) is a histologic diagnosis showing glandular and stromal hyperplasia in the prostate. Its symptoms usually occur after the age of 40, and its prevalence reaches 50%–60% by the age of 60 (1). About 50% of men who have a histologic diagnosis of BPH have lower urinary tract symptoms including storage and voiding symptoms (2). Imaging plays an important role in evaluation of enlargement locations and nodules, estimation of prostatic volumes, and management of BPH patients. Ultrasonography (US) and magnetic resonance imaging (MRI) are used in evaluation of the prostate. US is the most common imaging modality in BPH patients, because it is relatively inexpensive and provides important information in most patients. Recently, MRI has been more commonly used in management of prostate cancer (3).

Wasserman (4) described the US classification of BPH using findings on sagittal and axial images of transrectal US based on the pathologic classification (5). Following this, Wasserman et al. (6) implemented this classification to MRI. The classification for detecting BPH types is important, as patients with different BPH types may have different symptoms and treatment options.

In this paper, we retrospectively evaluated MRI scans of BPH patients who were histologically diagnosed as BPH and presented the different types of BPH on T2-weighted MRI, since the prostatic parenchyma is best evaluated on T2-weighted images (6, 7). Additionally, the sagittal and axial images that are important for the classification of BPH were only available on T2-weighted images. In our practice, we perform prostate MRI on a 3.0 T scanner (AchievaTX; Philips) using an endorectal coil (Prostate eCoil, Medrad).

Anatomy of the prostate

In previous studies (4, 8), the anatomy of the prostate has been reviewed. There are three main glandular zones (central, transition, peripheral) and one stromal zone (anterior fibromuscular stroma). There is also a subsphincteric periurethral gland (PUG) region, which is a fraction of the size of the transition zone (TZ) (9). BPH mostly involves PUGs, TZ, and stromal

zone (8). PUGs are located posterior to the proximal prostatic urethra and include two groups: a superficial group opening into the lumen and a deep group draining the ducts into the urethra. TZ is located anterolateral to the proximal urethra and superior to the verumontanum.

The proximal prostatic urethra is surrounded by the internal sphincter, which is composed of the smooth muscles of the bladder neck. The distal membranous urethra is surrounded by the external urethral sphincter, which is responsible for continence in men. The external urethral sphincter includes two muscular layers; the outer layer composed of striated muscles, and the inner layer composed of smooth muscles (10).

The anterior fibromuscular stroma, including fibromuscular extensions of the detrusor muscle, surrounds the prostate anterolaterally (11). There is also a capsule-like structure composed of fibromuscular tissue (mostly smooth muscle), which surrounds the entire prostate. The term "capsule" is an anatomic misnomer as this is not a real capsule that can be separated from the prostatic stroma. However, this term has been colloquially used (10).

Pathophysiology of benign prostatic hyperplasia

BPH includes glandular and stromal enlargements (12). Glandular enlargement mainly leads to the enlargement in the size of the prostate and obstructive symptoms, known as the static effect. Stromal enlargement increases the resistance of the parenchyma, known as the dynamic effect (4). BPH is characterized by expansile nodules, which include the proliferation of stroma, newly formed glandular structures, or both

Main points

- Benign prostatic hyperplasia (BPH) is a common condition in middle-aged and older men and may cause lower urinary tract symptoms which can affect the quality of life.

- We presented the types of BPH based on the magnetic resonance imaging (MRI) classification.

- The most common types of BPH were types 1 and 3 in the existing literature.

- MRI, with its superior soft tissue contrast resolution, is more advantageous than ultrasound in determination of stromal/glandular ratio and classification of BPH types which may potentially help in choosing optimal treatment.

of these (mixed type BPH nodule) (6). BPH nodules can be seen as ranging from hypointense to hyperintense on T2-weighted images depending on the ratio of stromal to glandular components (7). On T2-weighted images, the tissues with higher water content appear hyperintense, while those with less water content appear hypointense. Thus, hyperintense appearance (Fig. 1) of a BPH nodule is caused by cystic ectasia and hyperplastic glandular components, which are filled with secretion, while hypointense appearance (Fig. 2) is caused by fibromuscular components (13).

Enlargement in BPH patients occurs first in the PUGs in the fourth decade and then continues to the TZ, which is the main site of BPH (8). Although BPH mainly develops in TZ and PUGs, it can also develop in the peripheral zone (14). However, TZ enlargement typically compresses and decreases the volume of the peripheral zone in most BPH patients (6).

Magnetic resonance imaging classification of benign prostatic hyperplasia

MRI has been more commonly used in management of prostate cancer due to its better contrast resolution and sensitivity (3). Recent studies in the use of MRI for diagnosis of prostate cancer reported that MRI-based prostate volume-adjusted prostate-specific antigen (PSA) could improve the effectiveness of PSA in the diagnosis of prostate cancer, and MRI-US fusion biopsy could improve cancer detection in enlarged prostates (15, 16). Although US has been mainly performed in patients with BPH, MRI could be performed in patients with BPH due to in-
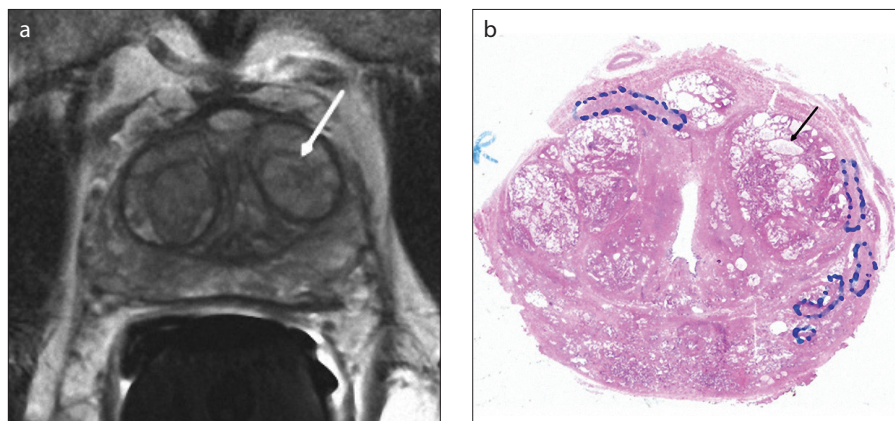

Figure 1. a, b. Axial T2-weighted image **(a)** of a 70-year-old male with type 3 BPH shows a predominantly hyperintense nodule *(arrow)* in the left transition zone. The pathology section **(b)** of this nodule is compatible with a mixed type BPH nodule consisting of mostly glandular components with markedly cystic glands *(arrow)*.
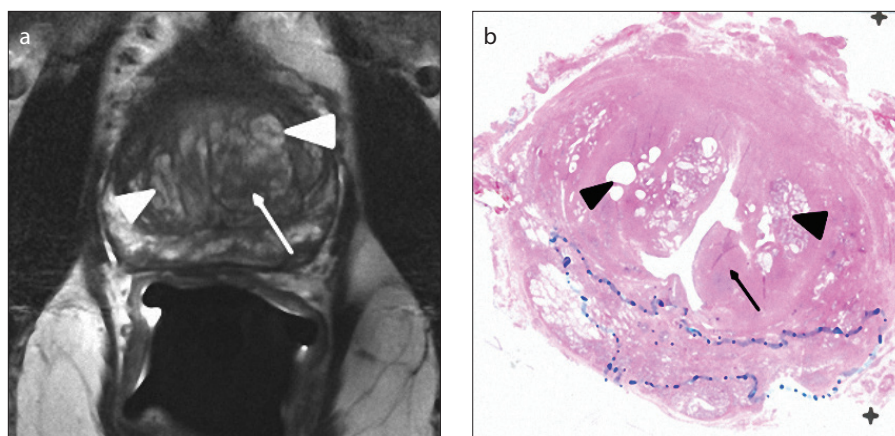

Figure 2. a, b. Axial T2-weighted image **(a)** of a 69-year-old male with type 3 BPH shows a hypointense area *(arrow)* in the left transition zone and bilateral predominantly hyperintense areas *(arrowheads)*. On the pathology section **(b)**, the hypointense area is compatible with a pure stromal BPH nodule *(arrow)*, and bilateral predominantly hyperintense areas are compatible with mixed type BPH nodules consisting of mostly glandular components with cystic glands *(arrowheads)*.
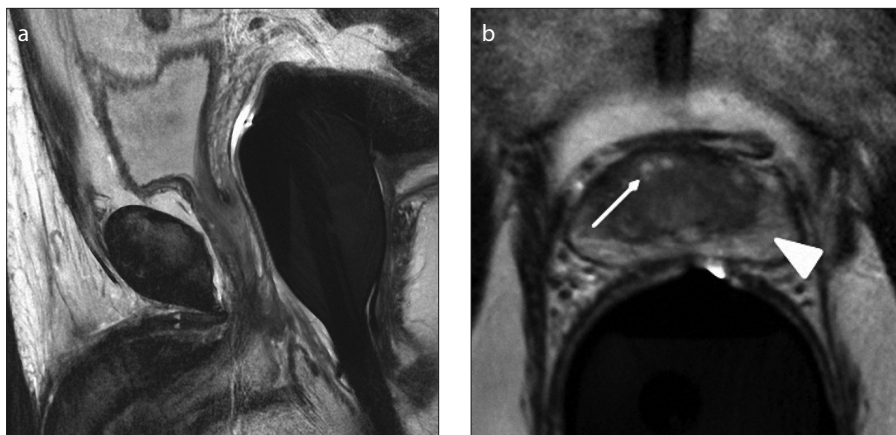
Figure 3. a, b. There is no marked prostatic enlargement on sagittal T2-weighted image **(a)** of a 43-year-old male with type 0 BPH. Axial T2-weighted image **(b)** shows mild heterogeneity *(arrow)* in the transition zone without any marked BPH nodules. Note that the peripheral zone *(arrowhead)* normally appears hyperintense on T2-weighted images.
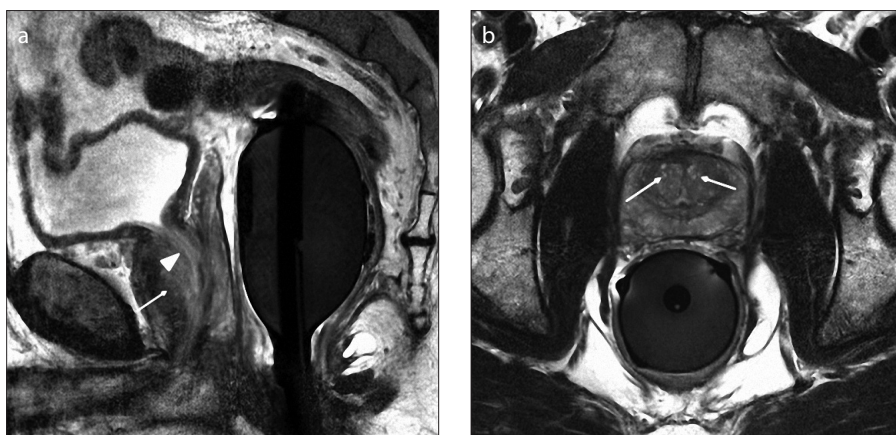

Figure 4. a, b. Sagittal T2-weighted image **(a)** of a 56-year-old male with type 1 BPH shows enlargement of transition zone *(arrow)*. Note that there is posterior displacement of urethra *(arrowhead)* due to BPH nodules. Axial T2-weighted image **(b)** shows enlargement of transition zone with bilateral BPH nodules *(arrows)*.
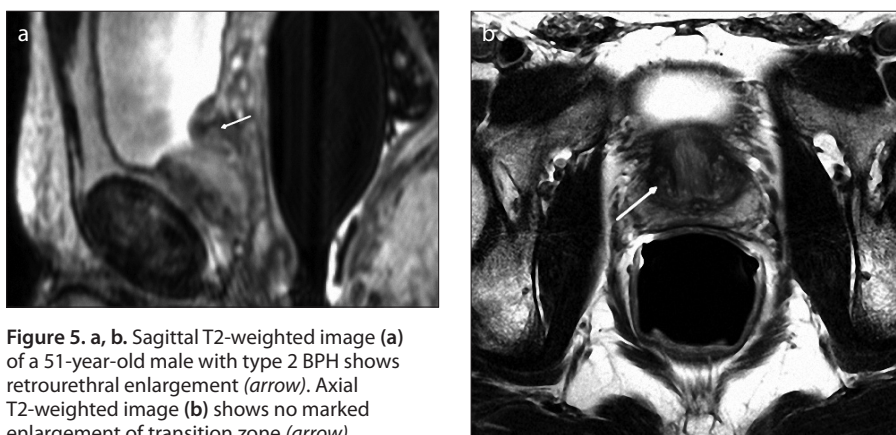

Figure 5. a, b. Sagittal T2-weighted image **(a)** of a 51-year-old male with type 2 BPH shows retrourethral enlargement *(arrow)*. Axial T2-weighted image **(b)** shows no marked enlargement of transition zone *(arrow)*.

creased PSA levels and suspected or known prostate cancer. MRI allows a secondary look at the BPH in these patients. Recently, the importance of MRI has been increasing in BPH patients, with potential uses including differentiation of BPH from prostate cancer,

estimation of zonal and entire prostatic volumes, detection of enlargement locations, and choosing optimal medical therapy based on the stromal/glandular ratio (3).

Randall (5) previously described a classification for BPH in 222 postmortem cases and

classified the enlarged regions of prostate. The types according to this classification are as follows: type 1, bilateral lobe enlargement; type 2, posterior commissural enlargement; type 3, bilateral and posterior commissural; type 4, subcervical; type 5, bilateral and subcervical; type 6, bilateral, posterior commissural and subcervical; type 7, anterior; and type 8, subtrigonal enlargement. Based on this classification, the US and MRI classifications of BPH were described (4, 6). BPH types on MRI are as follows: type 0, an equal to or less than 25 cm³ prostate showing little or no zonal enlargement (Fig. 3); type 1, bilateral TZ enlargement (35%); type 2, retrourethral enlargement (10%); type 3, bilateral TZ and retrourethral enlargement (46%); type 4, solitary or multiple pedunculated enlargement; type 5, pedunculated with bilateral TZ and/or retrourethral enlargement; type 6, subtrigonal or ectopic enlargement; and type 7, other combinations of enlargements.

Bilateral transition zone enlargement

The TZ margins appear more clearly with the enlargement, and the enlargement leads to the compression of the outer muscle layer of the urethra into a fibrostromal pseudo-capsule (the surgical capsule). Bilateral TZ enlargement is analogous to the enlargements of "right and left lateral lobes" in Randall's classification (5) and corresponds to type 1 in MRI classification (6) (Fig. 4). Bilateral TZ enlargement and BPH nodules are best evaluated on axial and coronal MRI scans.

Retrourethral enlargement

Randall (5) described the region posterior to the proximal urethra as posterior commissural (median), and it is regarded as retrourethral in MRI classification (6). Retrourethral enlargement arises from the deep PUGs. This type of enlargement may lead to bladder outlet obstruction by compressing the bladder and displacing the trigon superiorly. It is best evaluated on sagittal images due to the relationship between the trigon and retrourethral prostatic tissue.

Retrourethral enlargement alone is regarded as type 2 in MRI classification (6) (Fig. 5). Type 3 includes patients who exhibit both TZ and retrourethral enlargements (Fig. 6). Types 1 and 3 are the most common types seen (5).

Pedunculated enlargement

Randall (5) used the term "subcervical" enlargement for enlargement arising from the superficial PUGs in the posterior wall of

Figure 6. a, b. Sagittal T2-weighted image **(a)** of a 63-year-old male with type 3 BPH shows retrourethral enlargement *(arrow)*. Axial T2-weighted image **(b)** shows bilateral marked BPH nodules *(arrows)*.
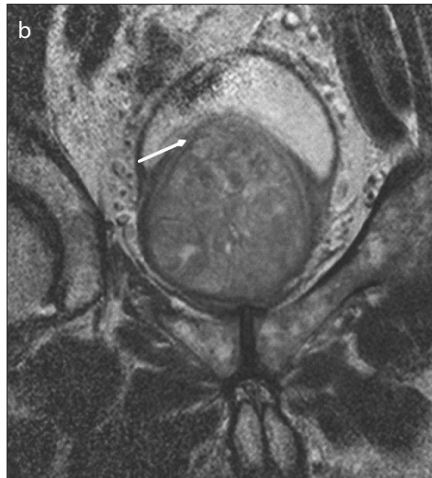

Figure 7. a, b. Sagittal T2-weighted image **(a)** of an 81-year-old male with type 5 BPH shows pedunculated enlargement *(arrow)* protruding into the bladder. Note that there is no displacement of trigon *(arrowhead)*. Coronal T2-weighted image **(b)** shows bladder compression *(arrow)* inferiorly and bilateral marked BPH nodules.

Figure 8. a, b. Sagittal T2-weighted image **(a)** of a 54-year-old male with type 5 BPH shows pedunculated enlargement *(arrow)* and superior displacement of trigon due to retrourethral enlargement *(arrowhead)*. Axial T2-weighted image **(b)** shows bilateral transition zone enlargement with BPH nodules *(arrows)*.

Figure 9. Sagittal T2-weighted image of a 54-year-old male with type 6 BPH shows subtrigonal enlargement *(arrow)* without marked displacement of trigon.

the proximal urethra. This corresponds to pedunculated enlargement in MRI classification (6) and is seen as an intravesicular prostatic protrusion above the urethra. In this type of enlargement, there are one or more than one lobulated enlarged prostatic nodules protruding directly into the bladder. In contrast to retrourethral enlargement, this type leads to bladder outlet obstruction without displacement of the trigon superiorly. It is best evaluated on sagittal images.

Pedunculated enlargement is more common in younger patients (5). Pedunculated enlargement alone is regarded as type 4 in MRI classification (6). Type 5 includes patients with pedunculated enlargements with TZ and/or retrourethral enlargements (Figs. 7 and 8).

Subtrigonal enlargement

An ectopic PUG enlargement may be seen in the subtrigonal region. Subtrigonal enlargement is usually oval- or round-shaped and limited to this region without any continuation inferiorly. This is a rare BPH type, and it is thought that this type may not usually lead to obstructive symptoms due to its relatively isolated location (4). This type is considered type 6 and is best evaluated on sagittal images (Fig. 9).

Type 7 includes patients exhibiting other combinations of these enlargements.

Conclusion

BPH is a common condition in middle-aged and older men and may cause lower urinary tract symptoms that can affect the quality of life. MRI, with its superior soft tissue contrast resolution, is more advantageous than US in differentiating BPH from prostate cancer, estimation of zonal and entire prostatic volumes, detection of enlargement locations, and classification of BPH types which may potentially help in choosing the optimal treatment. Thus, MRI can be effectively used for management of BPH in diagnosis, treatment, and response to the treatment.

Conflict of interest disclosure

The authors declared no conflicts of interest.

References

1. Berry SJ, Coffey DS, Walsh PC, Ewing LL. The development of human benign prostatic hyperplasia with age. J Urol 1984; 132:474–479.
2. Roehrborn CG, McConnell JD. Etiology, pathophysiology, epidemiology and natural history of benign prostatic hyperplasia. In: Walsh PC, Retik AB, Vaughn EB Jr, et al, eds. Campbell's urology. 8th ed. Philadelphia: WB Saunders Co., 2002; 1297–1330.
3. Grossfeld GD, Coakley FV. Benign prostatic hyperplasia: clinical overview and value of diagnostic imaging. Radiol Clin North Am 2000; 38:31–47. [CrossRef]
4. Wasserman NF. Benign prostatic hyperplasia: a review and ultrasound classification. Radiol Clin North AM 2006; 44:689–710. [CrossRef]
5. Randall A. Surgical pathology of prostatic obstructions. Baltimore: Williams & Wilkins, 1931.
6. Wasserman NF, Spilseth B, Golzarian J, Metzger GJ. Use of MRI for lobar classification of benign prostatic hyperplasia: potential phenotypic biomarkers for research on treatment strategies. AJR Am J Roentgenol 2015; 205:564–571. [CrossRef]
7. Ling D, Lee JK, Heiken JP, Balfe DM, Glazer HS, McClennan BL. Prostatic carcinoma and benign prostatic hyperplasia: inability of MR imaging to distinguish between the two diseases. Radiology 1986; 158:103–107. [CrossRef]
8. McNeal JE. Origin and evolution of benign prostatic enlargement. Invest Urol 1978; 15:340–345.
9. Selman SH. The McNeal prostate: a review. Urology 2011; 78:1224–1228. [CrossRef]
10. Walz J, Burnett AL, Costello AJ, et al. A critical analysis of the current knowledge of surgical anatomy related to optimization of cancer control and preservation of continence and erection in candidates for radical prostatectomy. Eur Urol 2010; 57:179–192. [CrossRef]
11. Oelrich TM. The urethral sphincter muscle in the male. Am J Anat 1980; 158:229–246. [CrossRef]
12. Marks LS, Treiger B, Dorey FJ, Fu YS, deKernion JB. Morphology of the prostate: distribution of tissue components in hyperplastic glands. Urology 1996; 44:486–492. [CrossRef]
13. Schiebler ML, Tomaszewski JE, Bezzi M, et al. Prostatic carcinoma and benign prostatic hyperplasia: correlation of high-resolution MR and histopathologic findings. Radiology 1989; 172:131–137. [CrossRef]
14. Aarnink RG, de la Rosette JJ, Huynen AL, Giesen RJ, Debruyne FM, Wijkstra H. Standardized assessment to enhance the diagnostic value of prostate volume; part I: morphometry in patients with lower urinary tract symptoms. Prostate 1996; 29:317–326. [CrossRef]
15. Peng Y, Shen D, Liao S, et al. MRI-based prostate volume-adjusted prostate-specific antigen in the diagnosis of prostate cancer. J Magn Reson Imaging 2015; 42:1733–1739. [CrossRef]
16. Walton Diaz A, Hoang AN, Turkbey B, et al. Can magnetic resonance-ultrasound fusion biopsy improve cancer detection in enlarged prostates? J Urol 2013; 190:2020–2025. [CrossRef]